Analysis of Ring-Stiffened Cylindrical Shells

Bingen Yang
Associate Professor,
Mechanical Engineering,
Mem. ASME.

Jianping Zhou[1]
Visiting Scholar.

University of Southern California,
Los Angeles, CA 90089-1453

A new analytical and numerical method is presented for modeling and analysis of cylindrical shells stiffened by circumferential rings. This method treats the shell and ring stiffeners as individual structural components, and considers the ring eccentricity with respect to the shell middle surface. Through use of the distributed transfer functions of the structural components, various static and dynamic problems of stiffened shells are systematically formulated. With this transfer function formulation, the static and dynamic response, natural frequencies and mode shapes, and buckling loads of general stiffened cylindrical shells under arbitrary external excitations and boundary conditions can be determined in exact and closed form. The proposed method is illustrated on a Donnell-Mushtari shell, and compared with finite element method and two other modeling techniques.

1 Introduction

Cylindrical shells stiffened by stringers and rings have wide engineering applications. The modeling techniques for such structure systems can be divided into two categories. The first category smears the stiffness of the stiffeners on the shell, and treats the stiffened shell as an orthotropic one; for instance, see Wang (1970) and the references therein. Such treatment is fine when the stiffeners are densely placed. However, if stiffeners are sparsely spaced that there are not enough stiffeners in each half wavelength in the circumferential and longitudinal directions of the shell, or if the actual deformation and stress distributions of the stiffened shell are needed, orthotropic approximation will loose accuracy. In this case, it is necessary to consider stiffeners as individual structural components, which gives rise to the second category of modeling techniques, namely, the analysis of combined shell-stiffener component systems.

Modeling stiffened cylindrical shells as combined component systems has been studied by many authors. Of various static and dynamic problems, free vibration of different stiffened shells has received great attention. Garnet and Goldberg (1962) and Godzvich and Ivanova (1965) considered ring-stiffened cylindrical shells. Schnell and Heinrichsbauer (1964) studied longitudinally stiffened thin-walled cylindrical shells. Egle and Sewall (1968) analyzed a ring-and-stringer-stiffened circular cylindrical shell by a Rayleigh-Ritz procedure. Wang and Rinehart (1974) modeled longitudinally stiffened cylindrical shells with arbitrary edge boundary conditions. Wang and Hsu (1985) proposed a model for stiffened composite cylindrical shells. Mead and Bardell (1987) investigated periodically stiffened cylindrical shells.

Among other problems, Wang and Lin (1973) examined the stability of stringer-stiffened cylindrical shells under axial pressure and simply supported boundary conditions; Reddy (1980) presented a bifurcation analysis for stringer-stiffened cylinders sustaining elastic-plastic deformation; and Sridharan et al. (1992) studied post-buckling of stiffened composite shells.

Several analytical and numerical methods for stiffened cylindrical shells have been developed. Forsberg (1969) obtained an exact solution for natural frequencies of ring-stiffened cylinders subjected to different boundary conditions. Al-Najafi and Warburton (1970) applied the finite element method to evaluate the natural frequencies and mode shapes of ring-stiffened cylindrical shells with each stiffening ring treated as a discrete element. Wang (1970) yielded a Fourier series solution of ring-and-stringer-stiffened cylindrical shells by treating the shell, rings, and stringers as structural components, and imposing deformation compatibility among those components. Wilken and Soedel (1976) used a receptance method to describe the modal characteristics of ring-stiffened shells. By Laplace transform and numerical inverse Laplace transform, Dekos and Oates (1981) predicted the dynamic response of ring-stiffened circular cylindrical shells subjected to axis-symmetric loading and boundary restriction conditions. Rigo (1992) developed the stiffened sheathing method and LBR-3 software for computing the response of orthotropic cylindrical shells. Combining wave propagation method and transfer matrix method, Huntington and Lyrintzis (1992) developed a modified wave method for analysis of skin-stringer panels which improves the numerical stability of transfer matrix method.

This paper proposes a new analytic and numerical method for constrained/combined, ring-stiffened cylindrical shells, which falls in the second category of modeling techniques. A typical example is shown in Fig. 1, where the shell consists of several serially connected segments of different geometry and material parameters, each shell segment may be constrained by springs and dampers that are circumferential distributed, the ring stiffeners are placed either inwardly, or outwardly, or symmetrically with respect to the shell middle surface, and the whole shell is subject to arbitrary external excitations and boundary conditions. The distributed transfer function formulation proposed in Yang (1992, 1994) is extended to model stiffened shells. In the analysis, the shell and stiffeners are modeled as individual structural components. Through both Fourier expansion and Laplace transform of the shell displacements, the initial and boundary value problem of the shell is cast into a spatial state-space form in the s-domain. The distributed transfer functions of the shell segments are then derived, based on which the shell and stiffeners are assembled by imposing displacement continuity and force balance on the shell-stiffener contact surface, leading to a global dynamic equilibrium equation. Solution of the equilibrium equation gives accurate estimation of the static deflection, natural frequencies and mode shapes, bucking loads, and forced response of stiffened cylindrical shells under arbitrary boundary conditions and external excitations.

The proposed method has the following advantages. First, the transfer function method provides exact and closed-form

[1] Currently at the National University of Defense Technology, China.

Contributed by the Applied Mechanics Division of THE AMERICAN SOCIETY OF MECHANICAL ENGINEERS for publication in the ASME JOURNAL OF APPLIED MECHANICS.

Discussion on this paper should be addressed to the Technical Editor, Professor Lewis T. Wheeler, Department of Mechanical Engineering, University of Houston, Houston, TX 77204-4792, and will be accepted until four months after final publication of the paper itself in the ASME JOURNAL OF APPLIED MECHANICS.

Manuscript received by the ASME Applied Mechanics Division, May 13, 1994; final revision, Sept. 23, 1994. Associate Technical Editor: J. N. Reddy.

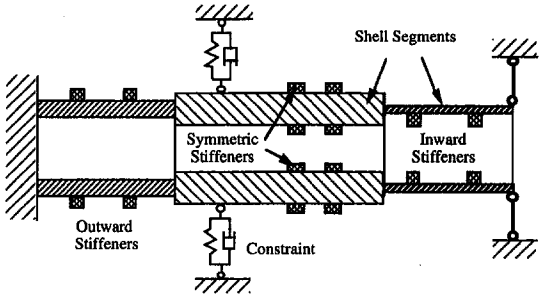

Fig. 1 A constrained/combined, ring-stiffened cylindrical shell

solutions for various static, dynamic, and control problems of stiffened cylindrical shells. Second, the transfer function method systematically treats different shell models (Love-Timoshenko or Donnell-Mushtari type, elastic or viscoelastic, stationary or spinning shells, etc.), and arbitrary boundary conditions and external excitations in a simple and unified manner, rendering numerical simulation and computer coding extremely convenient. Third, the transfer functions is especially capable of synthesizing combined cylindrical shells as shown in Fig. 1. All these will be demonstrated in the subsequent analysis and the numerical simulation.

2 Distributed Transfer Functions of Cylindrical Shells

The response of the homogeneous cylindrical shell in Fig. 2 is governed by

$$\sum_{k=1}^{3}\sum_{i=0}^{n_k}\sum_{j=0}^{i}\left[A_{mkij}\frac{\partial^2}{\partial t^2}+B_{mkij}\frac{\partial}{\partial t}+C_{mkij}\right]\frac{\partial^i u^k(x,\theta,t)}{\partial x^{i-j}\partial\theta^j}=f^m(x,\theta,t),\quad m=1,2,3 \tag{1}$$

where u^k ($k = 1, 2, 3$) are the shell displacements in the longitudinal (x-), circumferential (θ-) and radial (z-) coordinate directions, respectively, n_k is the highest order of differentiation of u^k, A_{mkij}, B_{mkij}, and C_{mkij} are constants of the shell, and $f^m(x, \theta, t)$ are the external loads acted on the shell. Here, Eq. (1) has been nondimensionalized so that $x = 0$ and $x = 1$ are the left and right boundaries of the shell. The boundary and initial conditions of the shell are

$$\left[\sum_{k=1}^{3}\sum_{i=0}^{n_k-1}\sum_{j=0}^{i}\beta_{lkij}\frac{\partial^i u^k(x_\alpha,\theta,t)}{\partial x^{i-j}\partial\theta^j}\right]_{x=x_\alpha}=\lambda^l(\theta,t),\quad l=1,2,\ldots,n_b \tag{2a}$$

and

$$u^k(x,\theta,t)|_{t=0}=u_0^k(x,\theta),\qquad \frac{\partial}{\partial t}u^k(x,\theta,t)\bigg|_{t=0}=u_0^{k,t}(x,\theta),\quad k=1,2,3 \tag{2b}$$

where $x_\alpha = 0$ and 1 for $\alpha = 1$ and 2, respectively, β_{lkij} are constants, and $\lambda^l(\theta, t)$, $u_0^k(x, \theta)$ and $u_0^{k,t}(x, \theta)$ are those proposed by given functions representing the boundary and initial disturbances. The number of boundary conditions $n_b = n_1 + n_2 + n_3$, and is 8 in most situations. Equations (1) and (2) represent many shell models, such as Donnell-Mushtari, Love-Timoshenko, Flugge-Novozhilov, Reissner, Vlasov, and Sanders.

To find the solution of the initial-boundary value problem formed by (1) and (2), the shell displacements and all the given functions of disturbances are expanded into Fourier series in circumferential direction θ

$$u^k(x,\theta,t)=\sum_{n=0}^{\infty}[u_{1,n}^k(x,t)\cos n\theta+u_{2,n}^k(x,t)\sin n\theta],\quad k=1,3 \tag{3a}$$

$$u^2(x,\theta,t)=\sum_{n=0}^{\infty}[u_{1,n}^2(x,t)\sin n\theta+u_{2,n}^2(x,t)\cos n\theta] \tag{3b}$$

$$f^m(x,\theta,t)=\sum_{n=0}^{\infty}[f_{1,n}^m(x,t)\cos n\theta+f_{2,n}^m(x,t)\sin n\theta],\quad m=1,2,3 \tag{3c}$$

$$u_0^k(x,\theta)=\sum_{n=0}^{\infty}[u_{1,n}^{k,0}(x)\cos n\theta+u_{2,n}^{k,0}(x)\sin n\theta],\quad k=1,3 \tag{3d}$$

$$u_0^2(x,\theta)=\sum_{n=0}^{\infty}[u_{1,n}^{2,0}(x)\sin n\theta+u_{2,n}^{2,0}(x)\cos n\theta] \tag{3e}$$

$$u_0^{k,t}(x,\theta)=\sum_{n=0}^{\infty}[u_{0,1,n}^{k,t}(x)\cos n\theta+u_{0,2,n}^{k,t}(x)\sin n\theta] \tag{3f}$$

$$u_0^{2,t}(x,\theta)=\sum_{n=0}^{\infty}[u_{0,1,n}^{2,t}(x)\sin n\theta+u_{0,2,n}^{2,t}(x)\cos n\theta] \tag{3g}$$

$$\lambda^l(\theta,t)=\sum_{n=0}^{\infty}[\lambda_{1,n}^l(t)\cos n\theta+\lambda_{2,n}^l(t)\sin n\theta],\quad l=1,2,\ldots,n_b. \tag{3h}$$

Here, the subscripts $(1, n)$ and $(2, n)$ indicate that the terms in Fourier series are related to $\cos n\theta$ and $\sin n\theta$, respectively. If all excitations are symmetric with respect to $\theta = 0$ and the shell is homogeneous and isotropic, each of the above Fourier series will only contain either cosine or sine- terms, thus reducing the number of unknowns by half.

Substituting the Fourier series into Eqs. (1) and (2), conducting Laplace transform with time t, and setting the coefficients of $\cos n\theta$ and $\sin n\theta$ to be equal on the both sides of the resulting equations, lead to an infinite number of equations ($m = 1, 2, 3$, $n = 0, 1, 2, \ldots$)

$$\sum_{k=1}^{3}\sum_{i=0}^{n_k}\left\{\sum_{j=0}^{[i/2]}D_{mki(2j)}(s)(-1)^j\frac{\partial^{i-2j}U_{1,n}^k}{\partial x^{i-2j}}+\sum_{j=1}^{[(i+1)/2]}D_{mki(2j-1)}(s)(-1)^{j+1}\frac{\partial^{i-(2j-1)}U_{2,n}^k}{\partial x^{i-(2j-1)}}\right\}=\tilde f_{1,n}^m(x,s)+\tilde g_{1,n}^m(x,s)$$

$$\sum_{k=1}^{3}\sum_{i=0}^{n_k}\left\{\sum_{j=0}^{[i/2]}D_{mki(2j)}(s)(-1)^j\frac{\partial^{i-2j}U_{2,n}^k}{\partial x^{i-2j}}+\sum_{j=1}^{[(i+1)/2]}D_{mki(2j-1)}(s)(-1)^j\frac{\partial^{i-(2j-1)}U_{1,n}^k}{\partial x^{i-(2j-1)}}\right\}=\tilde f_{2,n}^m(x,s)+\tilde g_{2,n}^m(x,s)$$

where $U_{j,n}^k = \tilde u_{j,n}^k$ for $k = 1$ and 3, and $U_{1,n}^2 = \tilde u_{2,n}^2$ and $U_{2,n}^2 = \tilde u_{1,n}^2$, $\tilde u_{i,n}^k$ and $\tilde f_{j,n}^m(x, s)$ are the Laplace transforms of $f_{j,n}^m(x, t)$

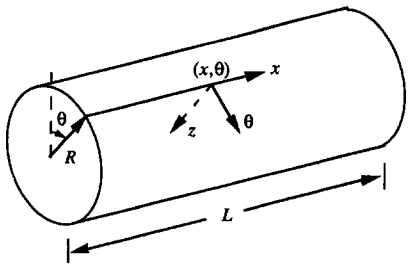

Fig. 2 A homogeneous cylindrical shell

and $u^k_{i,n}$, respectively; $\tilde{g}^m_{j,n}(x, s)$ are given in terms of $u^{k,0}_{j,n}(x)$; the complex numbers $D_{mkij}(s) = (A_{mkij}s^2 + B_{mkij}s + C_{mkij})n^j$; and s is the complex Laplace transform parameter. Note that the displacement functions $\tilde{u}^k_{i,n}$ and $\tilde{u}^k_{i,m}$ do not couple if n is not equal to m.

The above equations are cast in a state-space form

$$\frac{\partial \eta_n(x, s)}{\partial x} = F_n(s)\eta_n(x, s) + \tilde{f}_n(x, s) + \tilde{g}_n(x, s), \qquad n = 0, 1, \ldots \quad (4)$$

where the state-space vector contains the displacement functions $\tilde{u}^k_{i,m}$; i.e.,

$$\eta_n = \{\eta^T_{1,1,n} \quad \eta^T_{2,1,n} \quad \eta^T_{3,1,n} \quad \eta^T_{1,2,n} \quad \eta^T_{2,2,n} \quad \eta^T_{3,2,n}\}^T \in C^{2n_b} \quad (5a)$$

$$\eta_{k,i,n} = \left\{\tilde{u}^k_{i,n} \frac{\partial \tilde{u}^k_{i,n}}{\partial x} \cdots \frac{\partial^{n_k-1}\tilde{u}^k_{i,n}}{\partial x^{n_k-1}}\right\}^T \in C^{n_k}, \qquad k = 1, 2, 3, \quad i = 1, 2. \quad (5b)$$

$F_n(s)$ is a $2n_b \times 2n_b$ complex matrix containing the coefficients A_{mkij}, B_{mkij}, and C_{mkij} of (1), and the complex $2n_b$-vectors $\tilde{f}_n(x, s)$ and $\tilde{g}_n(x, s)$ are composed of $\tilde{f}^m_{j,n}(x, s)$ and $\tilde{g}^m_{j,n}(x, s)$, respectively. Similarly, the boundary conditions (2a) can be transformed into the form

$$M_n(s)\eta_n(0, s) + N_n(s)\eta_n(1, s) = \gamma_n(s) \quad (6)$$

where the boundary matrices $M_n(s)$ and $N_n(s)$ ($\in C^{2n_b \times 2n_b}$) contain the coefficients β_{lkij} in (2a), and the vector $\gamma_n(s)$ contain the Laplace transforms of the boundary excitation functions $\lambda^k_{j,m}$. One example of the above state-space form will be illustrated in Section 4.

The solution of the Eqs. (4) and (6) is (Yang and Tan, 1992)

$$\eta_n(x, s) = \int_0^1 G_n(x, \xi, s)(\tilde{f}_n(\xi, s) + \tilde{g}_n(\xi, s))d\xi + H_n(x, s)\gamma_n(s) \quad (7)$$

where the $2n_b \times 2n_b$ complex matrices

$$G_n(x, \xi, s) = \begin{cases} H_n(x, s)M_n(s)e^{-F_n(s)\xi}, & \xi \le x \\ -H_n(x, s)N_n(s)e^{F_n(s)(1-\xi)}, & \xi > x \end{cases} \quad (8a)$$

$$H_n(x, s) = e^{F_n(s)x}(M_n(s) + N_n(s)e^{F_n(s)})^{-1} \quad (8b)$$

are the distributed transfer functions of the shell. The displacement functions are found from η_n:

$$u^1(x, s) = \sum_{n=0}^{\infty} [\eta_{n,1}(x, s) \cos n\theta + \eta_{n,n_1+n_2+n_3+1}(x, s) \sin n\theta] \quad (9a)$$

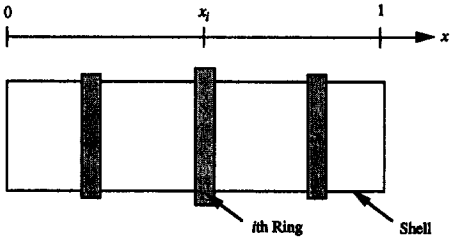

Fig. 3 A cylindrical shell stiffened by circumferential rings

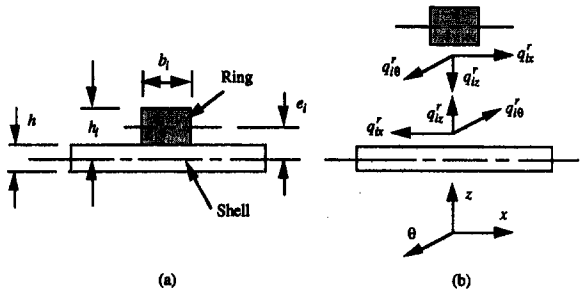

Fig. 4 Interaction between the shell and the ith ring: (a) geometry; (b) tractions

$$u^2(x, s) = \sum_{n=0}^{\infty} [\eta_{n,n_1+1}(x, s) \sin n\theta + \eta_{n,2n_1+n_2+n_3+1}(x, s) \cos n\theta] \quad (9b)$$

$$u^3(x, s) = \sum_{n=0}^{\infty} [\eta_{n,n_1+n_2+1}(x, s) \cos n\theta + \eta_{n,2n_1+2n_2+n_3+1}(x, s) \sin n\theta] \quad (9c)$$

where $\eta_{n,j}$ is the jth element of η_n.

In the above derivation, no approximation has been made; the transfer function formulation provides an exact and closed-form solution. The result here is quite general because different shell models and arbitrary boundary and initial conditions are dealt with by the same formula.

The transfer function formulation is directly applicable to the eigenvalue problems associated with free vibration and buckling of cylindrical shells, which are described by

$$[M_n(s; \bar{p}) + N_n(s; \bar{p})e^{F_n(s;\bar{p})}]\psi = 0 \quad (10)$$

with $\bar{p}$ being a load parameter and ψ a nonzero complex vector. The eigenvalues are the roots of the characteristic equation

$$\det [M_n(s; \bar{p}) + N_n(s; \bar{p})e^{F_n(s;\bar{p})}] = 0. \quad (11)$$

For free vibration of the shell, $\bar{p} = 0$ and s is the eigenvalue; the corresponding mode shape is determined by $\eta_n(x, s) = e^{F_n(s;0)x}\psi$ and (9). For a static buckling problem, $s = 0$ and $\bar{p}$ is the eigenvalue; the bucking mode shape is given by $\eta_n(x, \bar{p}) = e^{F_n(0;\bar{p})x}\psi$. For free vibration of a prestressed cylindrical shell, $\bar{p}$ is a nonzero constant and the s is the eigenvalue; the mode shape is given by $\eta_n(x, s) = e^{F_n(s;\bar{p})x}\psi$.

The transfer functions can also be used to determine the dynamic response and stability of the cylindrical shell under various forcing sources, and to design active vibration controllers and smart structure mechanism (Yang, 1994).

3 Analysis of Ring-Stiffened Cylindrical Shells

In Fig. 3, a homogeneous cylindrical shell is stiffened by N^r circumferential rings at $x = x_i$, $i = 1, \ldots, N^r$. Assume that the influence of the ring width is negligible. Denote the middle surface displacement of the ith ring by $u^r_{ik}(\theta, t)$, where the subscript refers to the ith stiffening ring, and the superscript r indicates that the parameters are related to the rings. The dynamic equations of the stiffening ring in general are

$$\sum_{k=1}^{3}\sum_{j=0}^{n_k}\left(\alpha_{imkj}\frac{\partial^2}{\partial t^2} + \beta_{imkj}\frac{\partial}{\partial t} + \gamma_{imkj}\right)\frac{\partial^j u^r_{ik}(\theta, t)}{\partial \theta^j} = q^r_{im} + q^e_{im} \quad (12)$$

where $m = 1, 2, 3$, $i = 1, \ldots, N^r$, the constants α_{imkj}, β_{imkj}, and γ_{imkj} are related to the geometry and material parameters of the rings, and q^e_{im} are the external loads applied to the ith ring. Here q^r_{im} are the tractions between the shell and the ith ring; see Fig. 4, where $q^r_{i1} = q^r_{ix}$, $q^r_{i2} = q^r_{i\theta}$ and $q^r_{i3} = q^r_{iz}$. Like

Eq. (1), (12) is quite general and represents many different curved beam models.

For thin-walled cylindrical shells, the Kirchhoff hypothesis holds and the displacements of the shell and rings satisfy the following matching conditions:

$$u^r_{i1}(\theta, t) = [u^1 - e_i u,^3_x]_{x=x_i} \tag{13a}$$

$$u^r_{i2}(\theta, t) = \left[u^2 - e_i \frac{1}{R} u,^3_\theta\right]_{x=x_i} \tag{13b}$$

$$u^r_{i3}(\theta, t) = u^3(x_i, \theta, t) \tag{13c}$$

where $u,^3_x = \partial u^3/\partial x$, $u,^3_\theta = \partial u^3/\partial\theta$, and e_i is the eccentricity of the centroid of the ith stiffening ring from the middle surface of the shell; see Fig. 4(a). The e_i is positive (negative or zero) if the ring is inward (outward or symmetric).

The analysis of the stiffened shell follows three steps: Fourier expansion, Laplace transform, and state-space formulation. The Fourier series of the displacements and loads are

$$u^r_{ik}(\theta, t) = \sum_{n=0}^{\infty} [u^{i,k}_{r,1,n}(t) \cos n\theta + u^{i,k}_{r,2,n}(t) \sin n\theta], \quad k = 1, 3 \tag{14a}$$

$$u^r_{i,2}(\theta, t) = \sum_{n=0}^{\infty} [u^{i,2}_{r,1,n}(t) \sin n\theta + u^{i,2}_{r,2,n}(t) \cos n\theta] \tag{14b}$$

$$q^r_{ik}(\theta, t) = \sum_{n=0}^{\infty} [q^{i,k}_{r,1,n}(t) \cos n\theta + q^{i,k}_{r,2,n}(t) \sin n\theta], \quad k = 1, 2, 3 \tag{14c}$$

$$q^e_{ik}(\theta, t) = \sum_{n=0}^{\infty} [q^{i,k}_{e,1,n}(t) \cos n\theta + q^{i,k}_{e,2,n}(t) \sin n\theta], \quad k = 1, 2, 3. \tag{14d}$$

Substituting (3a, b), (14a, b) into (12) and (13), one has

$$\begin{aligned} q^{i,m}_{r,1,n} \cos n\theta + q^{i,m}_{r,2,n} \sin n\theta &= -q^{i,m}_{r,1,n} \cos n\theta - q^{i,m}_{r,2,n} \sin n\theta \\ &+ \sum_{k=1}^{3} \sum_{j=0}^{n_k} \left(\alpha_{imkj} \frac{\partial^2}{\partial t^2} + \beta_{imkj} \frac{\partial}{\partial t} + \gamma_{imkj}\right) \frac{\partial^j u^k_n}{\partial \theta^j}\bigg|_{x=x_i} \\ &- \frac{ne_i}{R} \sum_{j=0}^{n_2} \left(\alpha_{im2j} \frac{\partial^2}{\partial t^2} + \beta_{im2j} \frac{\partial}{\partial t} + \gamma_{im2j}\right) \frac{\partial^j}{\partial \theta^j} \\ &\times (u^3_{2,n} \cos n\theta - u^3_{1,n} \sin n\theta)|_{x=x_i} - e_i \\ &\times \sum_{j=0}^{n_1} \left(\alpha_{im1j} \frac{\partial^2}{\partial t^2} + \beta_{im1j} \frac{\partial}{\partial t} + \gamma_{im1j}\right) \\ &\times \frac{\partial}{\partial x} \frac{\partial^j}{\partial \theta^j} (u^3_{1,n} \cos n\theta + u^3_{2,n} \sin n\theta)|_{x=x_i} \end{aligned} \tag{15}$$

for $m = 1, 2$ and 3, where n is the circumferential wave number of the shell. Laplace transform of (15) and application of the state-space form (4) lead to

$$\tilde{q}^{r,n}_i(s) = L^{i,n}(s)\eta_n(x_i, s) - \tilde{q}^{e,n}_i(s) \tag{16}$$

where $\tilde{q}^{r,n}_i(s)$ is the vector of the tractions between the shell and rings, $\tilde{q}^n_i(s)$ is the vector of the external loads, including the initial disturbances, and the matrix $L^{i,n}(s)$ consists of the parameters of the ith ring (see the Appendix).

Since the traction forces $\tilde{q}^{r,n}_i$ are pointwise along the x-direction, the total forces π_n applied to the shell can be expressed by

$$\pi_n(x, s) = \hat{f}_n(x, s) + \sum_{i=1}^{N^r} T^r_i L^{i,n}(s)\eta_n(x_i, s)\delta(x - x_i) \tag{17}$$

where $\delta(x - x_i)$ is the delta function, $\hat{f}_n(x, s)$ is the resultant of the external loads on the shell and rings, and the equivalent forces due to the initial disturbances of the rings, T^r_i are scaling matrices guaranteeing the same dimension of $\tilde{q}^{r,n}_i$ in (16) and $\tilde{f}_n$ in (4). By (4), we have

$$\eta_n(x, s) = e^{F_n(s)x}\left\{\int_0^x e^{-F_n(s)\xi}[\pi_n(\xi, s) + \tilde{g}_n(\xi, s)]d\xi + \eta_n(0, s)\right\}. \tag{18}$$

Substituting (17) into the above gives

$$\eta_n(x, s) = A^{(0)}_n(x, s) + \sum_{j=1}^{N^r} B_{n,j}(x, s)\eta_n(x_j, s) + C^{(0)}_n(x, s)\eta_n(0, s) \tag{19}$$

where

$$A^{(0)}_n(x, s) = e^{F_n(s)x} \int_0^x e^{-F_n(s)\xi}[\hat{f}_n(\xi, s) + \tilde{g}_n(\xi, s)]d\xi$$

$$B_{n,j}(x, s) = e^{F_n(s)(x-x_j)} T^r_i L^{j,n}(s) u(x - x_j), \quad j = 1, \ldots, N^r$$

$$C^{(0)}_n(x, s) = e^{F_n(s)x}$$

and $u(x - x_j)$ is the unit step function. Eliminating $\eta_n(x_j, s)$ from (19) by setting $x = x_i$, $i = 1, \ldots, N^r$, and solving the N^r resulting equations yield

$$\eta_n(x, s) = \bar{A}_n(x, s) + \bar{C}_n(x, s)\eta_n(0, s) \tag{20}$$

where the matrices $\bar{A}_n(x, s)$ and $\bar{C}_n(x, s)$ are obtained from the N^r-step recurrence procedure

$$A^{(i)}_n(x, s) = A^{(i-1)}_n(x, s) + B_{n,i}(x, s)[I - B_{n,i}(x_i, s)]^{-1} A^{(i-1)}_n(x_i, s) \tag{21a}$$

$$C^{(i)}_n(x, s) = C^{(i-1)}_n(x, s) + B_{n,i}(x, s)[I - B_{n,i}(x_i, s)]^{-1} C^{(i-1)}_n(x_i, s) \tag{21b}$$

for $i = 1, 2, \ldots, N^r$, with $\bar{A}_n(x, s) = A^{(N^r)}_n(x, s)$ and $\bar{C}_n(x, s) = C^{(N^r)}_n(x, s)$.

Finally, by plugging (20) into the boundary conditions (6), we obtain the response of the ring-stiffened cylindrical shell under various external loads, and initial and boundary conditions

$$\eta_n(x, s) = \bar{A}_n(x, s) + \bar{C}_n(x, s)[M_n(s) + N_n(s)\bar{C}_n(1, s)]^{-1} \times [\gamma_n(s) - N_n(s)\bar{A}_n(1, s)]. \tag{22}$$

For the eigenvalue problems of the stiffened shell, the characteristic equation by (22) is

$$\det [M_n(s; \bar{p}) + N_n(s; \bar{p})\bar{C}_n(1, s; \bar{p})] = 0 \tag{23}$$

and the discussion after Eq. (11) applies.

Constrained cylindrical shells can be viewed as the degenerate cases of stiffened shells. Assume that the shell is constrained by N^s pairs of uniformly distributed springs and dampers, located at $x = x_i$ ($i = 1, \ldots, N^s$) and along the circle $0 \le \theta \le 2\pi$. At $x = x_i$, the constraint forces by the springs and dampers are described by

$$\begin{Bmatrix} q^s_{i1} \\ q^s_{i2} \\ q^s_{i3} \end{Bmatrix} = -\left(K_i + D_i \frac{\partial}{\partial t}\right) \begin{Bmatrix} u^1 - \bar{u}^1 \\ u^2 - \bar{u}^2 \\ u^3 - \bar{u}^3 \end{Bmatrix}_{x=x_i}$$

where the matrices K_i and D_i contain the spring and damper coefficients, respectively, and the $\bar{u}^j$ count for the unstretched status of the springs. It can be shown that the matrix $L^{i,n}(s)$ in (16) is expressed in terms of the elements of $K_i + sD_i$. The response of the constrained shell can be determined based on (21) and (22).

In summary, the distributed transfer function analysis of the ring-stiffened shell follows three steps: (a) for given shell and ring parameters and boundary conditions, form the state-space matrices $F_n(s)$, $M_n(s)$, $N_n(s)$, and $L^{i,n}(s)$; (b) determine $\bar{A}_n(x, s)$ and $\bar{C}_n(x, s)$ by the recurrence procedure (21); and (c) evaluate the response of the shell by (22).

The result herein can be applied to stepped cylindrical shells stiffened by circumferential rings. A stepped shell is composed of a number of serially connected uniform shell segments. The analysis for such structures first obtains the distributed transfer functions and response of each stiffened shell segment based on (22), and then assembles all the shell segments by a synthesis given in our recent paper (Zhou and Yang, 1995).

4 Donnell-Mushtari Shell

As an application of the theory developed, free vibration of the Donnell-Mushtari shell is considered. Without loss of generality, assume that the shell is homogeneous, isotropic, and elastic. The dimensionless equations of motion are (Markus, 1988)

$$\frac{1}{\gamma_1^2}\frac{\partial^2 u}{\partial x^2} + \frac{1}{2}(1-\upsilon)\frac{\partial^2 u}{\partial \theta^2} + \frac{1+\upsilon}{2\gamma_1}\frac{\partial^2 \upsilon}{\partial x \partial \theta} - \frac{\upsilon}{\gamma_1}\frac{\partial w}{\partial x} = \bar{\rho}\frac{\partial^2 u}{\partial t^2} \quad (24a)$$

$$\frac{1+\upsilon}{2\gamma_1}\frac{\partial^2 u}{\partial x \partial \theta} + \frac{1-\upsilon}{2\gamma_1^2}\frac{\partial^2 \upsilon}{\partial x^2} + \frac{\partial^2 \upsilon}{\partial \theta^2} - \frac{\partial w}{\partial \theta} = \bar{\rho}\frac{\partial^2 \upsilon}{\partial t^2} \quad (24b)$$

$$\frac{\upsilon}{\gamma_1}\frac{\partial u}{\partial x} + \frac{\partial \upsilon}{\partial \theta} - w - k\left(\frac{1}{\gamma_1^4}\frac{\partial^4 w}{\partial x^4} + \frac{2}{\gamma_1^2}\frac{\partial^4 w}{\partial x^2 \partial \theta^2} + \frac{\partial^4 w}{\partial \theta^4}\right) + \frac{1}{J}\left(N_{x0}\frac{\partial^2 w}{\gamma_1^2 \partial x^2} + 2N_{x\theta 0}\frac{\partial^2 w}{\gamma_1 \partial x \partial \theta} + N_{\theta 0}\frac{\partial^2 w}{\partial \theta^2}\right) = \bar{\rho}\frac{\partial^2 w}{\partial t^2} \quad (24c)$$

with

$$(u, \upsilon, w) = \frac{1}{h}(u_0, \upsilon_0, w_0), \quad k = \frac{1}{12}\left(\frac{h}{R}\right)^2,$$

$$\bar{\rho} = \frac{\rho(1-\upsilon^2)R^2}{E}, \quad \gamma_1 = \frac{L}{R}, \quad J = \frac{Eh}{1-\upsilon^2}.$$

Here u_0, υ_0, and w_0 are the displacements of the shell middle surface in the coordinate directions x, θ, and z, respectively; R, L, and h are the radius, length, and thickness of the shell, respectively; E and ν are Young's modulus and Poison's ratio; ρ is the density per unit volume; and N_{x0}, $N_{\theta 0}$ and $N_{x\theta 0}$ are the membrane stresses.

Four pairs of boundary conditions are as follows:

(i) $u(\bar{x}_i, \theta, t) = 0$ or

$$\frac{E}{1-\upsilon^2}\frac{h^2}{R}\left[\frac{1}{\gamma_1}u_{,x} + \upsilon(\upsilon_{,\theta} - w)\right]_{x=\bar{x}_i} = 0 \quad (25a)$$

(ii) $\upsilon(\bar{x}_i, \theta, t) = 0$ or

$$\frac{E}{2(1+\upsilon)}\frac{h^2}{R}\left[u_{,\theta} + \frac{1}{\gamma_1}\upsilon_{,x} + \frac{2k}{\gamma_1}w_{,x\theta}\right]_{x=\bar{x}_i} = 0 \quad (25b)$$

(iii) $w(\bar{x}_i, \theta, t) = 0$ or

$$-\frac{E}{12(1-\upsilon^2)}\frac{h^4}{R^3}\left[\frac{1}{\gamma_1^3}w_{,xxx} + \frac{2-\upsilon}{\gamma_1}w_{,x\theta\theta}\right]_{x=\bar{x}_i} = 0 \quad (25c)$$

(iv) $w_{,x}|_{x=\bar{x}_i} = 0$ or

$$-\frac{E}{12(1-\upsilon^2)}\frac{h^4}{R^2}\left[\frac{1}{\gamma_1^2}w_{,xx} + \upsilon w_{,\theta\theta}\right]_{x=\bar{x}_i} = 0 \quad (25d)$$

where $\bar{x}_i = 0$ and 1 for $i = 1$ and 2, and $u_{,x} = \partial u/\partial x$, etc.

The Fourier series of the shell displacements are written as

$$u = \sum_{n=0}^{\infty} u_n(x, t)\cos n\theta, \quad \upsilon = \sum_{n=0}^{\infty} \upsilon_n(x, t)\sin n\theta,$$

$$w = \sum_{n=0}^{\infty} w_n(x, t)\cos n\theta. \quad (26)$$

Following the procedure outlined in Section 2, η_n and F_n in (4) are found as

$$\eta_n(x, s) = \left\{\tilde{u}_n \frac{\partial \tilde{u}_n}{\partial x}\ \tilde{\upsilon}_n \frac{\partial \tilde{\upsilon}_n}{\partial x}\ \tilde{w}_n \frac{\partial \tilde{w}_n}{\partial x}\ \frac{\partial^2 \tilde{w}_n}{\partial x^2}\ \frac{\partial^3 \tilde{w}_n}{\partial x^3}\right\},$$

$$F_n(s) = \begin{bmatrix} F_{11} & F_{12} \\ F_{21} & F_{22} \end{bmatrix} \quad (27)$$

where

$$F_{11}(s) = \begin{bmatrix} 0 & 1 & 0 & 0 \\ \gamma_1^2\left(\frac{1-\nu}{2}n^2 + s^2\bar{\rho}\right) & 0 & 0 & -\frac{1+\upsilon}{2}n\gamma_1 \\ 0 & 0 & 0 & 1 \\ 0 & \gamma_1 n\frac{1+\upsilon}{1-\upsilon} & \frac{2n^2\gamma_1^2}{1-\upsilon} + \frac{2\bar{\rho}s^2\gamma_1^2}{1-\upsilon} & 0 \end{bmatrix}$$

$$F_{12}(s) = \begin{bmatrix} 0 & 0 & 0 & 0 \\ 0 & \upsilon\gamma_1 & 0 & 0 \\ 0 & 0 & 0 & 0 \\ -\frac{2n\gamma_1^2}{1-\upsilon} & 0 & 0 & 0 \end{bmatrix} \quad F_{21} = \begin{bmatrix} 0 & 0 & 0 & 0 \\ 0 & 0 & 0 & 0 \\ 0 & 0 & 0 & 0 \\ 0 & \gamma_1^3\frac{\upsilon}{k} & \frac{n\gamma_1^4}{k} & 0 \end{bmatrix}$$

$$F_{22} = \begin{bmatrix} 0 & 1 & 0 & 0 \\ 0 & 0 & 1 & 0 \\ 0 & 0 & 0 & 1 \\ -\gamma_1^4\left(\frac{1}{k} + n^4 + \frac{\bar{\rho}}{k}s^2\right) & -\frac{n^2\gamma_1^4 N_{\theta 0}}{kJ} & -\frac{2n\gamma_1^3 N_{x\theta 0}}{kJ} & 2n^2\gamma_1^2 + \frac{\gamma_1^2 N_{x0}}{kJ} & 0 \end{bmatrix}.$$

By (25), (26), and (27), η_n must satisfy the boundary conditions

$$B_i\Gamma_n\eta_n(\bar{x}_i, s) = 0, \quad i = 1, 2 \quad (28)$$

where

$$\Gamma_n = \begin{bmatrix} 1 & 0 & 0 & 0 & 0 & 0 & 0 & 0 \\ 0 & 1/\gamma_1 & n\upsilon & 0 & -\upsilon & 0 & 0 & 0 \\ 0 & 0 & 1 & 0 & 0 & 0 & 0 & 0 \\ -n & 0 & 0 & 1/\gamma_1 & 0 & -kn/(6\gamma_1) & 0 & 0 \\ 0 & 0 & 0 & 0 & 1 & 0 & 0 & 0 \\ 0 & 0 & 0 & 0 & 0 & -(2-\upsilon)n^2/\gamma_1 & 0 & 1/\gamma_1^3 \\ 0 & 0 & 0 & 0 & 0 & 1 & 0 & 0 \\ 0 & 0 & 0 & 0 & -\upsilon n^2 & 0 & 1/\gamma_1^2 & 0 \end{bmatrix} \quad (29)$$

and B_i is a 4×8 matrix containing 1 or 0. Write $B_i = [B_i(j, k)]$. Define the Kronecker delta by $\delta_m^k = 1$ for $k = m$ and 0 for $k \neq m$. If the kth boundary condition is of displacement type ($u = 0$, or $v = 0$, or $w = 0$, or $w_{,x} = 0$), the nonzero elements of the kth row of B_i are

$$B_i(j, 2j-1) = \delta_{2j-1}^k. \quad (30a)$$

If the kth boundary condition is of force type ($N_x = 0$, or $N_{x\theta} = 0$, $Q_x = 0$, or $M_x = 0$), then the nonzero element of the kth row of B_i is given by

$$B_i(j, k) = \delta_{2j}^k. \quad (30b)$$

The boundary matrices in (6) take the form

$$M_n(s) = \begin{bmatrix} B_1 L_n \\ 0_{4\times 8} \end{bmatrix} \quad N_n(s) = \begin{bmatrix} 0_{4\times 8} \\ B_2 L_n \end{bmatrix}. \quad (31)$$

The displacements u_i^r, v_i^r, and w_i^r of the ith stiffening ring are governed by

$$q_{ix}^r + q_{ix}^e = \rho_i A_i \frac{\partial^2 u_i^r}{\partial t^2} \quad (32a)$$

$$\frac{1}{R}\frac{\partial N_{i\theta}^r}{\partial \theta} + q_{i\theta}^r + q_{i\theta}^e = \rho_i A_i \frac{\partial^2 v_i^r}{\partial t^2} \quad (32b)$$

$$\frac{1}{R^2}\frac{\partial^2 M_{i\theta}^r}{\partial \theta^2} + \frac{N_{i\theta}^r}{R} + N_{\theta 0}\frac{\partial^2 w_i^r}{\partial \theta^2} + q_{iz}^r = \rho_i A_i \frac{\partial^2 w_i^r}{\partial t^2} \quad (32c)$$

where ρ_i and A_i are the density and the cross section area of the ith ring, respectively, and the superscript r indicates that the physical parameters are related to the ring. Here the middle surface of the shell has been chosen as the reference plane. The internal forces of the ring are related to the shell displacements by

$$N_{i\theta}^r = k_{11}^i\left(-\frac{w}{R} + \frac{1}{R}\frac{\partial v}{\partial \theta}\right) - k_{12}^i\frac{\partial^2 w}{R^2\partial\theta^2} \quad (33a)$$

$$M_{i\theta}^i = k_{12}^i\left(-\frac{w}{R} + \frac{1}{R}\frac{\partial v}{\partial \theta}\right) - k_{22}^i\frac{\partial^2 w}{R^2\partial\theta^2} \quad (33b)$$

where the coordinate z is measured from the middle surface of the shell,

$$k_{11}^i = E_i A_i, \quad k_{12}^i = E_i A_i e_i, \quad k_{22}^i = E_i I_{i\rho}, \quad (34)$$

and e_i is the eccentricity of the ring centroid shown (see Fig. 4(a)), and $I_{i\rho}$ is the second-order moment of the ring cross section with respect to the middle surface of the shell.

The key in estimating the response of the stiffened shell is to determine the matrix $L^{i,n}(s)$ in (16), whose nonzero elements $L_{j,l}^{i,n}$ are obtained as follows:

$$L_{2,1}^{i,n} = \bar{k}R^2\rho_i A_i\gamma_1^2 s^2, \quad L_{2,6}^{i,n} = -\bar{k}R^2\rho_i A_i\gamma_1^2 e_i s^2,$$

$$L_{4,3}^{i,n} = (n^2 k_{11}^i + \rho_i A_i R^2 s^2)\frac{2\bar{k}\gamma_1^2}{1-\upsilon}$$

$$L^{i,n}_{4,5} = -\left(nk^i_{11} - \frac{n^3k^i_{12}}{R} - n\rho_i A_i R s^2 e_i\right)\frac{2\bar{k}\gamma_1^2}{1-\upsilon},$$

$$L^{i,n}_{8,3} = \left(nk^i_{11} - \frac{n^3k^i_{12}}{R}\right)\frac{\bar{k}\gamma_1^4}{k}$$

$$L^{i,n}_{8,5} = -\left(k^i_{11} - \frac{2}{R}k^i_{12}n^2 + \frac{n^4k^i_{22}}{R^2} + n^2N_{\theta 0} + R^2\rho_i A_i s^2\right)\frac{\bar{k}\gamma_1^4}{k}$$

with $\bar{k} = (1-\upsilon^2)/(Eh^2)$.

For the comparison purpose, the stiffened cylindrical shell is also approximated as an orthotropic shell by smearing the tension and bending stiffness of the rings on the shell. The internal force-strain relations in this case are given by

$$\begin{Bmatrix} N_x \\ N_\theta \\ N_{x\theta} \end{Bmatrix} = \frac{Eh}{1-\upsilon^2}\begin{bmatrix} 1 & \upsilon & 0 \\ \upsilon & 1+\Delta D_t & 0 \\ 0 & 0 & \dfrac{1-\upsilon}{2} \end{bmatrix}\begin{Bmatrix} \epsilon_{x0} \\ \epsilon_{\theta 0} \\ \epsilon_{x\theta 0} \end{Bmatrix} + \Delta B_{tb}\begin{Bmatrix} 0 \\ \kappa_\theta \\ 0 \end{Bmatrix} \quad (35a)$$

$$\begin{Bmatrix} M_x \\ M_\theta \\ M_{x\theta} \end{Bmatrix} = \frac{Eh^3}{12(1-\upsilon^2)}\begin{bmatrix} 1 & \upsilon & 0 \\ \upsilon & 1+\Delta D_b & 0 \\ 0 & 0 & 1-\upsilon \end{bmatrix}\begin{Bmatrix} \kappa_x \\ \kappa_\theta \\ \kappa_{x\theta} \end{Bmatrix} + \Delta B_{tb}\begin{Bmatrix} 0 \\ \epsilon_\theta \\ 0 \end{Bmatrix} \quad (35b)$$

where

$$\Delta D_t = \frac{1}{EhL}(1-\upsilon^2)\sum_{i=1}^{N^r} k^i_{11},$$

$$\Delta D_b = \frac{12}{Eh^3L}(1-\upsilon^2)\sum_{i=1}^{N^r} k^i_{22}, \quad \Delta B_{tb} = \frac{1}{L}\sum_{i=1}^{N^r} k^i_{12}.$$

For the shell simply supported ($N_x = \upsilon = w = M_x = 0$) at its both ends, the frequency equation is

$$\det(A + \omega^2 I) = 0 \quad (36)$$

where

$$A = \frac{E}{\bar{\rho}(1-\upsilon^2)R^2}\begin{bmatrix} -\left(\dfrac{m^2\pi^2}{\gamma_1^2} + \dfrac{1-\upsilon}{2}n^2\right) & \dfrac{1+\upsilon}{2\gamma_1}nm\pi & -\dfrac{\upsilon}{\gamma_1}m\pi \\ \dfrac{1+\upsilon}{2\gamma_1}nm\pi & -\left(\dfrac{1-\upsilon}{2\gamma_1^2}m^2\pi^2 + (1+\Delta D_t)n^2\right) & n(1+\Delta D_t) - \Delta\bar{B}_{tb}n^3 \\ -\dfrac{\upsilon}{\gamma_1}m\pi & n(1+\Delta D_t) - \Delta\bar{B}_{tb}n^3 & \bar{A}^{33}_{mn} \end{bmatrix}$$

with

$$\Delta\bar{B}_{tb} = \frac{\Delta B_{tb}(1-\upsilon^2)}{EhRL}, \quad \bar{\rho} = \rho + \frac{1}{Lh}\sum_{i=1}^{N^r}\rho_i b_i h_i$$

Table 1 The fundamental frequency of the cylindrical shell with inward stiffeners

N^r	Proposed Method	Orthotropic Approximation
1	0.2699(6)	0.2622(6)
2	0.2777(6)	0.2711(6)
3	0.2849(6)	0.2791(6)
4	0.2914(6)	0.2863(6)
5	0.2974(6)	0.2927(6)
6	0.3028(6)	0.2985(6)
7	0.3048(5)	0.3038(6)
8	0.3053(5)	0.3051(5)
9	0.3058(5)	0.3056(5)
10	0.3061(5)	0.3060(5)

$$\bar{A}^{33}_{mn} = -\left[1 + \Delta D_t - 2n^2\Delta\bar{B}_{tb} + k\left(\frac{m^4\pi^4}{\gamma_1^4} + \frac{2n^2m^2\pi^2}{\gamma_1^2} + n^4(1+\Delta D_b)\right)\right].$$

5 Numerical Results

Consider a Donnell-Mushtari shell stiffened by N^r identical rings that are equally spaced along the longitudinal direction x. The parameters of the shell and stiffening rings are chosen as

Shell: $R = L = 100, \quad h = 1, \quad E = 10^4, \quad \upsilon = 0.3$

Rings: $E_i = 10^4, \quad \upsilon_i = 0.3, \quad b_i = 1, \quad h_i = 2$

where b_i and h_i are the width and height of the rings, as shown in Fig. 4(*a*). The shell is simply supported at the both ends; i.e., $N_x = \upsilon = w = M_x = 0$ at $x = 1$ and 100.

The natural frequencies of the ring-stiffened shell are determined by four methods: (i) the proposed transfer function method (23); (ii) the orthotropic approximation (36); (iii) the stepped shell modeling given by Zhou and Yang (1995); and (iv) the finite element method. It should be noted that the last two methods are only valid for shells with symmetric stiffeners, i.e., the stiffener eccentricity e_i in Fig. 4(*a*) is zero. In this case, with each ring and the connecting shell segment taken as a short cylindrical shell, the whole stiffened shell becomes a stepped shell, which, accordingly, can be analyzed by the stepped shell synthesis and the finite element method. However, if inward or outward stiffeners are used (see Fig. 1), the shell can not be modeled as a stepped shell because the middle surfaces of those short shells do not coincide; the stepped shell assumption in Methods (iii) and (iv) may lead to inaccurate results.

Table 2 The fundamental frequency of the cylindrical shell with outward stiffeners

N^r	Proposed Method	Orthotropic Approximation
1	0.2670(6)	0.2617(6)
2	0.2742(6)	0.2702(6)
3	0.2814(6)	0.2777(6)
4	0.2881(6)	0.2844(6)
5	0.2940(6)	0.2905(6)
6	0.2993(6)	0.2960(6)
7	0.3040(6)	0.3009(6)
8	0.3083(6)	0.3054(6)
9	0.3102(5)	0.3094(6)
10	0.3108(5)	0.3106(5)

Shown in Tables 1 and 2 is the fundamental (lowest) natural frequency of the cylindrical shell with inward and outward stiffening rings, respectively, with the number N^r of the stiffeners varying from 1 to 10. The results obtained by the proposed method and the orthotropic approximation are in good agreement in all the cases. This is expected because the frequency is a global parameter and the orthotropic stiffness treatment is accurate enough for the frequency calculation if the stiffeners are densely spaced. However, it is impossible for the orthotropic approximation to predict the kinks and jumps in the distributions of the stresses or internal forces of the stiffened shell, as shall be seen in Figs. 5–8.

For the shell with symmetric stiffeners, its fundamental (lowest) natural frequency is calculated by the aforementioned four methods; see Table 3. It is seen that the frequency predicted by the first two methods is lower than that by the last two, especially for a larger N^r. This is mainly due to the fact that the stiffener width b_i, and therefore the tension and bending stiffness of the rings in the longitudinal direction are ignored in the proposed method and the orthotropic approximation. In all three tables, the digit in the brackets is the circumferential wave number n corresponding to the lowest natural frequency.

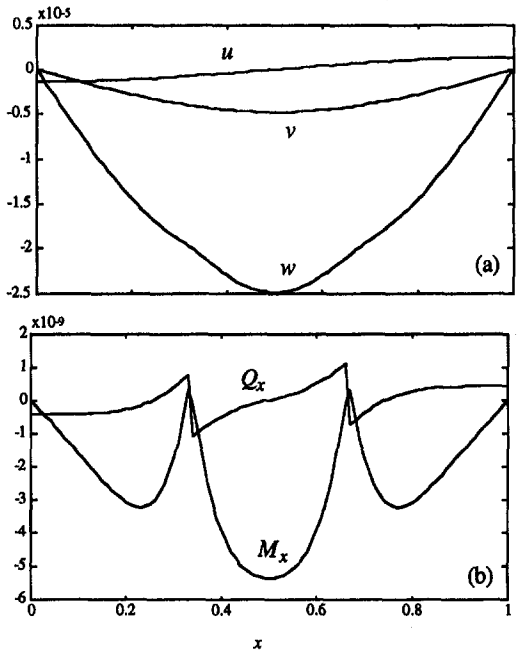

Fig. 6 Eigenfunctions of the shell with two symmetric stiffeners (N^r = 2, fundamental frequency = 0.2602): (*a*) mode shapes; (*b*) moment and shear force

The mode shapes (u, v, w), and the distributions of the bending moment (M_x) and shear force (Q_x) of the stiffened shell are plotted in Figs. 5 to 8 by the proposed transfer function method, corresponding to the fundamental frequency in Table 3 for N^r = 1, 2, 3, 4. The rings have most significant effect on the transverse displacement w and almost no effect on the longitudinal displacement u. The kinks in the M_x-plots and jumps in the Q_x are clearly seen, which can not be obtained by the orthotropic approximation. As N^r increases, more kinks and

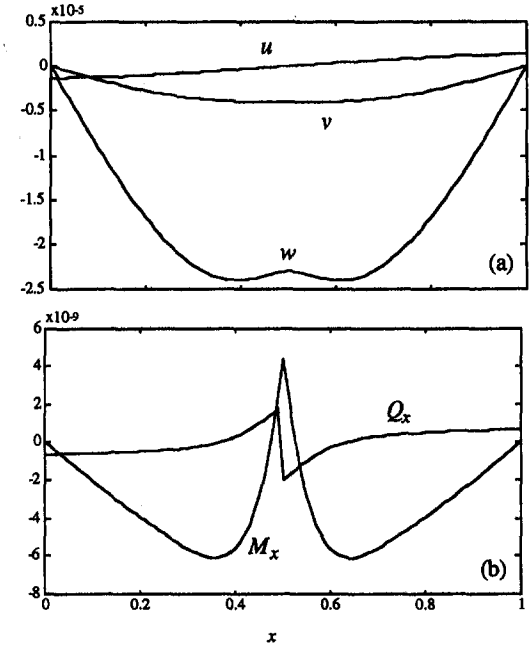

Fig. 5 Eigenfunctions of the shell with one symmetric stiffener (N^r = 1, fundamental frequency = 0.2567): (*a*) mode shapes; (*b*) moment and shear force

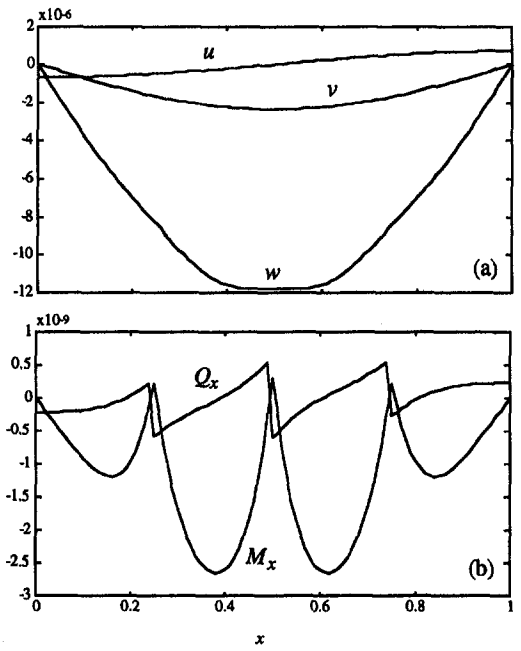

Fig. 7 Eigenfunctions of the shell with three symmetric stiffeners (N^r = 3, fundamental frequency = 0.2627): (*a*) mode shapes; (*b*) moment and shear force

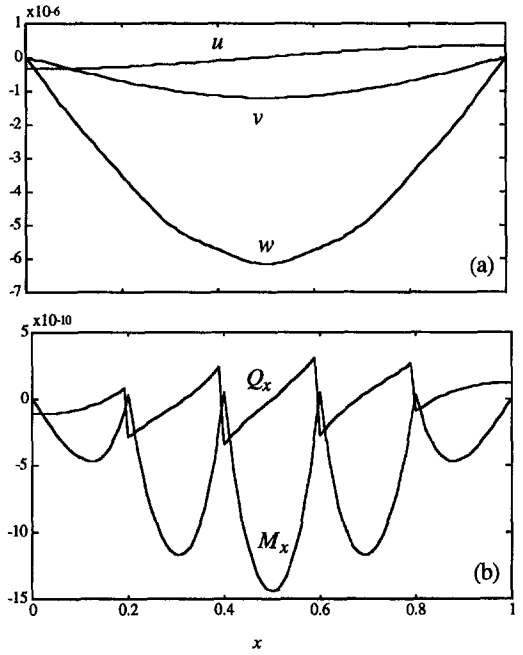

Fig. 8 Eigenfunctions of the shell with four symmetric stiffeners (N^r = 4, fundamental frequency = 0.2650): (*a*) mode shapes; (*b*) moment and shear force

jumps occur in the moment and shear force curves near the locations of the stiffeners.

6 Conclusions

We have analyzed cylindrical shells stiffened by circumferential rings. The shell and stiffening rings are modeled as individual structural components. By Fourier expansion, Laplace transform, and a spatial state-space formalism, the distributed transfer functions of the shell and rings are determined in exact and closed form. By imposing force balance and displacement compatibility among the structural components, the contact forces between the shell and stiffening rings are expressed in terms of the shell displacements by the transfer functions. In this way a general formulation for exact solution of various static and dynamic problems for constrained/combined, stiffened cylindrical shells is obtained.

The proposed transfer function method provides a systematic way to study ring-stiffened cylindrical shells; the solution procedure is the same for different shell models, stiffening conditions, initial and boundary conditions, and external loads. Consequently, the method is very convenient in computer coding and numerical simulation.

The numerical simulation on the free vibration of the stiffened Donnell-Mushtari shell reveals the following:

(i) If the number of the stiffeners is small, the stiffener positions have great influence on the shell response. If the number of stiffeners is large enough, smearing the stiffener stiffness on the shell is a good approximation for natural frequency calculation, but it is not accurate in estimating the stress/internal force distributions.

(ii) The stiffener eccentricity has significance influence on the natural frequencies and the dynamic behavior of the stiffened shell.

It should be noted that the current investigation takes into consideration the ring eccentricity and ring position with respect to the shell middle surface, which are difficult to depict in many modeling techniques. The transfer function method developed in this paper can easily handle inward, outward and symmetric ring stiffeners.

Table 3 The fundamental frequency of the cylindrical shell with symmetric stiffeners

N^r	Proposed Method	Orthotropic Approximation	Stepped Shell Synthesis	Finite Element Method
1	0.2567(7)	0.2497(7)	0.2571(7)	0.2542(7)
2	0.2602(6)	0.2570(7)	0.2631(6)	0.2606(6)
3	0.2627(7)	0.2603(6)	0.2676(6)	0.2650(6)
4	0.2650(6)	0.2627(6)	0.2720(6)	0.2692(6)
5	0.2672(6)	0.2650(6)	0.2762(6)	0.2733(6)
6	0.2693(6)	0.2672(6)	0.2804(6)	0.2772(6)
7	0.2714(6)	0.2693(6)	0.2843(6)	0.2810(6)
8	0.2733(6)	0.2714(6)	0.2881(6)	0.2847(6)
9	0.2752(6)	0.2733(6)	0.2918(6)	0.2882(6)
10	0.2770(6)	0.2752(6)	0.2953(6)	0.2915(6)

Acknowledgments

This work was partially supported by the U.S. Army Research Office under Grant No. DAAL03-93-G-0066 with Dr. Gary Anderson as the technical monitor.

References

Al-Najafi, A. M., and Warburton, G. B., 1970, "Free Vibration of Ring-Stiffened Cylindrical Shells," *Journal of Sound and Vibration,* Vol. 13, No. 1, pp. 9–25.

Deskos, D. E., and Oates, J. B., 1981, "Dynamic Analysis of Ring-Stiffened Circular Cylindrical Shells," *Journal of Sound and Vibration,* Vol. 75, No. 1, pp. 1–15.

Egle, D. M., and Sewall, J. L., 1968, "An Analysis of Free Vibration of Orthogonally Stiffened Cylindrical Shells with Stiffeners Treated as Discrete Elements," *AIAA Journal,* Vol. 6, No. 3, pp. 518–526.

Frosberg, K., 1969, "Exact Solution For Natural Frequencies of Ring-Stiffened Cylinders," *AIAA/ASME 10th Structures, Structural Dynamics and Materials Conference,* Volume on Structures and Materials, pp. 18–30.

Garnet, H., and Goldberg, M. A., 1962, "Free Vibrations of Ring-Stiffened Shells," RE-156, Grumman Aircraft Research.

Godzevich, V. G., and Ivanova, O. V., 1965, "Free Oscillations of Circular Conical and Cylindrical Shell Reinforced by Rigid Circular Ribs," TTF-291, NASA.

Huntington, D. E., and Lyrintzis, C. S., 1992, "Dynamics of Skin-Stringer Panels Using Modified Wave Methods," *AIAA Journal,* Vol. 30, No. 11, pp. 2765–2773.

Markus, S., 1989, *The Mechanics of Vibrations of Cylindrical Shells,* Elsevier, Amsterdam.

Mead, D. J., and Bardell, N. S., 1987, "Free Vibration of a Thin Cylindrical Shell with Periodic Circumferential Stiffeners," *Journal of Sound and Vibration,* Vol. 115, No. 3, pp. 499–520.

Reddy, B. D., 1980, "Buckling of Elastic-Plastic Discretely Stiffened Cylinders in Axial Compression," *International Journal of Solid and Structures,* Vol. 16, pp. 313–328.

Rigo, P., 1992, "Stiffened Sheathings of Orthotropic Cylindrical Shells," *Journal of Structural Engineering,* Vol. 118, No. 4, pp. 926–943.

Schnell, W., and Heinrichsbauer, F. J., 1964, "The Determination of Free Vibrations of Longitudinally Stiffened Thin-Walled Circular Shells," TTF-8856, NASA.

Soedel, W., 1981, *Vibrations of Shells and Plates,* Marcel Dekker, New York.

Sridharan, S., Zeggane, M., and Starnes, Jr., J. H., 1992, "Postbuckling Response of Stiffened Composite Cylindrical Shells," *AIAA Journal,* Vol. 30, No. 12, pp. 2897–2905.

Wang, J. T. S., 1970, "Orthogonally Stiffened Cylindrical Shells Subjected to Internal Pressure," *AIAA Journal,* Vol. 8, No. 3, pp. 455–461.

Wang, J. T. S., and Lin, Y. J., 1973, "Stability of Discretely Stringer-Stiffened Cylindrical Shells," *AIAA Journal,* Vol. 11, No. 6, pp. 810–813.

Wang, J. T. S., and Rinehart, S. A., 1974, "Free Vibrations of Longitudinally Stiffened Cylindrical Shells," ASME JOURNAL OF APPLIED MECHANICS, Vol. 41, No. 4, pp. 1087–1093.

Wang, J. T. S., and Hsu, T. M., 1985, "Discrete Analysis of Stiffened Composite Cylindrical Shells," *AIAA Journal,* Vol. 23, No. 11, pp. 1753–1761.

Wilken, I. D., and Soedel, W., 1976, "The Receptance Method Applied to Ring-Stiffened Cylindrical Shells: Analysis of Model Characteristics," *Journal of Sound and Vibration,* Vol. 44, No. 4, pp. 563–576.

Yang, B., 1992, "Transfer Functions of Constrained/Combined One-Dimensional Continuous Dynamic Systems," *Journal of Sound and Vibration,* Vol. 156, No. 3, pp. 425–443.

Yang, B., and Tan, C. A., 1992, "Transfer Functions of One Dimensional Distributed Parameter Systems," ASME JOURNAL OF APPLIED MECHANICS, Vol. 59, No. 4, pp. 1009–1014.

Yang, B., 1994, "Distributed Transfer Function Analysis of Complex Distributed Parameter Systems," ASME JOURNAL OF APPLIED MECHANICS, Vol. 61, No. 1, pp. 84–92.

Zhou, J., and Yang, B., 1995, "A Distributed Transfer Function Method for Analysis of Cylindrical Shells," *AIAA Journal,* Vol. 33, No. 9, pp. 1698–1708.

APPENDIX

Define

$$d_{mkij}(s) = \alpha_{mkij}s^2 + \beta_{mkij}s + \gamma_{mkij}$$

$$l_{1m} = \sum_{j=1}^{m} n_j, \quad l_{2m} = n_1 + n_2 + n_3 + \sum_{j=1}^{m} n_j.$$

Let δ_j^i be Kronecker delta. Let $[y]$ be the integer part of the number y. Denote the elements of $L^{i,n}(s)$ by $L_{j,k}^{i,n}$, $j, k = 1, \ldots, 2n_b$. The nonzero elements of $L^{i,n}(s)$ are as follows:

$$L_{l_{1m},l}^{i,n} = \delta_l^{l_{1k}} \sum_{j=0}^{[n_k/2]} d_{imk(2j)}s(-1)^j n^{2j} - \delta_l^{2n_1+2n_2+2n_3} \frac{ne_i}{R} \{ \sum_{j=0}^{[n_2/2]} d_{im2(2j)}(s)(-1)^j n^{2j} \}$$

$$L_{l_{1m},l}^{i,n} = \delta_l^{l_{2k}} \sum_{j=1}^{[(n_k+1)/2]} d_{imk(2j-1)}(s)(-1)^{j+1} n^{2j-1} - \delta_l^{n_1+n_2+n_3} \frac{ne_i}{R} \{ \sum_{j=1}^{[(n_2+1)/2]} d_{im2(2j-1)}(s)(-1)^j n^{2j-1} \}$$

$$L_{l_{2m},l}^{i,n} = \delta_l^{l_{1k}} \sum_{j=1}^{[(n_k+1)/2]} d_{imk(2j-1)}(s)(-1)^j n^{2j-1} - \delta_l^{2n_1+2n_2+2n_3} \frac{ne_i}{R} \{ \sum_{j=1}^{[(n_k+1)/2]} d_{im2(2j-1)}(s)(-1)^j n^{2j-1} \}$$

$$L_{l_{2m},l}^{i,n} = \delta_l^{l_{2k}} \sum_{j=0}^{[n_k/2]} d_{imk(2j)}(s)(-1)^j n^{2j} - \delta_l^{n_1+n_2+n_3} \frac{ne_i}{R} \{ \sum_{j=0}^{[n_2/2]} d_{im2(2j)}(-1)^{j+1} n^{2j} \}$$

$$L_{l_{2m},n_1+n_2+n_3}^{i,n} = -e_i \sum_{j=1}^{[(n_1+1)/2]} d_{im1(2j-1)}(s)(-1)^j n^{2j-1}$$

$$L_{l_{2m},2n_1+2n_2+2n_3}^{i,n} = -e_i \sum_{j=0}^{[n_1/2]} d_{im1(2j)}(s)(-1)^j n^{2j}$$

$$L_{l_{2m},n_1+n_2+n_3}^{i,n} = -e_i \sum_{j=1}^{[(n_1+1)/2]} d_{im1(2j-1)}(s)(-1)^j n^{2j-1}$$

$$L_{l_{2m},2n_1+2n_2+2n_3}^{i,n} = -e_i \sum_{j=0}^{[n_1/2]} d_{im1(2j)}(s)(-1)^j n^{2j}.$$